

fluorosulfonic acid (4 drops) and ca. 4 mg of antimony pentafluoride. The yellow solution was stirred at  $-78\text{ }^{\circ}\text{C}$  for 15 min and then poured into a solution of sodium methoxide in methanol at  $-78\text{ }^{\circ}\text{C}$ . The solution was allowed to warm to room temperature, diluted with water, and extracted with methylene chloride ( $3 \times 30\text{ mL}$ ). The dried extracts were concentrated and purified by preparative thin-layer chromatography (elution with 5% ethyl acetate in petroleum ether). There was isolated 0.4 mg (12%) of **32** and 2.2 mg (61%) of **39**: IR ( $\text{CHCl}_3$ ) 2930, 1270, 910,  $900\text{ cm}^{-1}$ ;  $^1\text{H NMR}$  (300 MHz,  $\text{CDCl}_3$ )  $\delta$  3.50-3.37 (m, 16 H), 3.37 (s, 3 H), 3.24 (s, 3 H);  $^{13}\text{C NMR}$  (125 MHz,  $\text{CDCl}_3$ ) 68.90, 66.90, 66.79, 65.77, 65.48, 51.19 ppm (1 C not observed); MS,  $m/z$  ( $\text{M}^+$ ) calcd 290.1670, obsd 290.1678.

**B. Treatment of 32 with Silver Triflate in the Presence of Methanol.** Bromide **32** (1.0 mg, 0.0030 mmol) was dissolved in methylene chloride (2 mL) and methanol (2 mL) and treated with silver trifluoromethanesulfonate (5.0 mg, 0.023 mmol). The mixture was stirred at ambient temperature in the dark for 18 h. Methylene chloride (15 mL) was added, and the organic phase was washed with water (2 $\times$ ) and dried. The solid obtained after concentration was purified by preparative TLC. Elution with 5% ethyl acetate in petroleum ether afforded **39** (0.6 mg, 69.8%), identical in all respects to the material obtained in part A.

**Dodecahedranol (40b).**<sup>49</sup> To **1** (3.9 mg, 0.015 mmol) dissolved in dry dichloromethane (1 mL) was added an excess amount of lead tetraacetate (ca. 10 mg) followed by trifluoroacetic acid (1 mL) and a small amount of dry lithium chloride. The resulting suspension was stirred in the dark for 24 h at room temperature. The reaction mixture was diluted with ether (20 mL) and water (5 mL), the layers were separated, and the aqueous phase was further extracted with ether ( $3 \times 20\text{ mL}$ ). The combined organic phases were washed with water (2 $\times$ ) and saturated sodium bicarbonate solution (1 $\times$ ) prior to drying. Filtration and solvent removal gave trifluoroacetate **40a** which was taken up in benzene (2 mL) and heated to  $100\text{ }^{\circ}\text{C}$  for 2 h in the presence of 10% sodium hydroxide solution (2 mL). The cooled mixture was diluted with water (10 mL) and extracted with dichloromethane ( $3 \times 30\text{ mL}$ ). The combined extracts were washed with water and dried. Solvent removal gave a white solid which was triturated with ether (2 $\times$ ) leaving pure **40b** (3.1 mg, 75.6%): mp  $>250\text{ }^{\circ}\text{C}$  (sealed tube);  $^1\text{H NMR}$  (300 MHz,  $\text{CDCl}_3$ )  $\delta$  3.55 (br s, 6 H), 3.35 (br s, 10 H), 3.26-3.20 (m, 3 H), 1.76 (s, 1 H);  $^{13}\text{C NMR}$  (75 MHz,  $\text{CDCl}_3$ ) 115.99, 74.95, 66.97, 66.89, 65.71 (2 C) ppm; MS,  $m/z$  ( $\text{M}^+$ ) calcd 276.1515, obsd 276.1482.

**Alternative Synthesis of (Trifluoroacetoxy)dodecahedrane (40a).**<sup>49</sup> Bromododecahedrane (**32**; 9.0 mg, 0.027 mmol) was dissolved in tri-

fluoroacetic acid (5 mL), treated with silver trifluoroacetate (20 mg, 0.09 mmol), and stirred at room temperature for 20 h. The trifluoroacetic acid was evaporated in vacuo, and dichloromethane (15 mL) was added to the residue. The organic phase was washed with water (2 $\times$ ) and brine (1 $\times$ ) prior to drying. Solvent removal yielded a solid which was passed through a short silica gel column. Elution with benzene furnished 7.9 mg (84.0%) of **40a** as a white solid: mp  $183\text{--}185\text{ }^{\circ}\text{C}$ , dec  $220\text{ }^{\circ}\text{C}$  (from hexane); IR ( $\text{CHCl}_3$ ) 2940, 1730, 1355, 1340, 1305, 1300, 1230,  $1160\text{ cm}^{-1}$ ;  $^1\text{H NMR}$  (300 MHz,  $\text{CDCl}_3$ )  $\delta$  3.58 (br s, 9 H), 3.40 (s, 10 H);  $^{13}\text{C NMR}$  (75 MHz,  $\text{CDCl}_3$ ) 126.47, 71.65, 66.69, 66.51, 65.90, 65.34 ppm (2 C of ester group not observed); MS,  $m/z$  ( $\text{M}^+ - \text{CF}_3\text{CO}_2\text{H}$ ) calcd 258.1408, obsd 258.1407.

**Dodecahedryl Nitrate (41).** Dodecahedrane (3.4 mg, 0.013 mmol) was taken up in deuteriochloroform (3 mL) under an argon atmosphere and treated with an excess of commercial nitronium tetrafluoroborate. The heterogeneous mixture was stirred vigorously for 68 h and then diluted with dichloromethane and water. The layers were separated, and the aqueous phase was further extracted with dichloromethane ( $3 \times 20\text{ mL}$ ). The combined organic extracts were washed with brine and dried. Filtration and removal of solvent gave a yellow solid which was passed through a plug of silica gel (elution with dichloromethane). Recrystallization from ethyl acetate yielded 3.5 mg (83.5%) of **41** as colorless crystals: mp  $220\text{ }^{\circ}\text{C}$  dec; IR ( $\text{CHCl}_3$ ) 3060, 2950, 1615, 1300,  $1270\text{ cm}^{-1}$ ;  $^1\text{H NMR}$  (300 MHz,  $\text{CDCl}_3$ ) 129.89, 70.33, 66.67, 66.47, 65.94, 65.19 ppm; MS (CI)  $m/z$  320 ( $\text{M}^+ - 1$ , 1.57), 275 ( $\text{M}^+ - \text{NO}_2$ , 10.45), 259 ( $\text{M}^+ - \text{ONO}_2$ , 100).

**N-Dodecahedrylacetamide (42).**<sup>49</sup> Bromododecahedrane (**32**; 10.3 mg, 0.0304 mmol) was heated at reflux in acetonitrile (10 mL) containing silver trifluoromethanesulfonate (150 mg) in the dark for 20 h. After cooling, water (10 mL) was added and the solution was stirred for 15 min prior to extraction with dichloromethane ( $3 \times 30\text{ mL}$ ). The combined extracts were washed with brine and dried. Filtration and solvent removal gave 9.6 mg (99.6%) of **42** as a white solid: mp  $>250\text{ }^{\circ}\text{C}$  (from ethyl acetate); IR ( $\text{CHCl}_3$ ) 2950, 1660,  $1490\text{ cm}^{-1}$ ;  $^1\text{H NMR}$  (300 MHz,  $\text{CDCl}_3$ )  $\delta$  5.81 (br s, 1 H), 3.55 (br s, 6 H), 3.37 (s, 3 H), 3.37-3.28 (m, 10 H), 1.92 (s, 3 H);  $^{13}\text{C NMR}$  (125 MHz,  $\text{CDCl}_3$ ) 168.95, 95.77, 74.21, 66.80, 66.80, 66.68, 66.16, 66.07, 23.80 ppm; MS,  $m/z$  ( $\text{M}^+$ ) calcd 317.1780, obsd 317.1772.

**Acknowledgment.** We are grateful to the National Institutes of Health for their generous financial support of this research program (Grant AI-11490).

## The Dodecahedryl Cation and 1,16-Dodecahedryl Dication. $^1\text{H}$ and $^{13}\text{C}$ NMR Spectroscopic Studies and Theoretical Investigations<sup>1a</sup>

George A. Olah,\*<sup>†</sup> G. K. Surya Prakash,<sup>†</sup> Wolf-Dieter Fessner,<sup>†</sup> Tomoshige Kobayashi,<sup>‡,1b</sup> and Leo A. Paquette\*<sup>‡</sup>

Contribution from the Donald P. and Katherine B. Loker Hydrocarbon Research Institute and Department of Chemistry, University of Southern California, Los Angeles, California 90089-1661, and Evans Chemical Laboratories, The Ohio State University, Columbus, Ohio 43210. Received June 13, 1988

**Abstract:** Ionization of dodecahedryl derivatives (**4**, X = Cl, OH) as well as of the parent hydrocarbon **1** itself under superacidic conditions ( $\text{SbF}_5/\text{SO}_2\text{ClF}$ ) gave the dodecahedryl cation, **2**, which was found to be a static ion with no tendency to undergo degenerate hydrogen scrambling (on the NMR time scale) up to  $0\text{ }^{\circ}\text{C}$ . The unique ion **2** was characterized by  $^1\text{H}$  and  $^{13}\text{C}$  NMR spectroscopy. Upon prolonged exposure to the superacidic medium, the dodecahedryl cation was irreversibly transformed into the 1,16-dodecahedryl dication, **3**, which opens up the possibility for regioselective difunctionalization of the dodecahedrane sphere. According to semiempirical SCF-MO calculations, the dodecahedrane skeleton is incapable of accommodating a planar cation geometry. This situation is still more acute in dication **3**, which is considered to constitute the first true  $\text{sp}^3$ -hybridized carbocation. Likewise, the static nature of these cations is shown to be due to unfavorable bending in the transition state for intramolecular 1,2-hydride shifts on the convex surface of the cage.

The formidable challenge<sup>2</sup> of synthesizing the pentagonal dodecahedrane **1**, a  $\text{C}_{20}\text{H}_{20}$  hydrocarbon of spherical polycyclopentanoic topology (composed of 12 five-membered rings) with

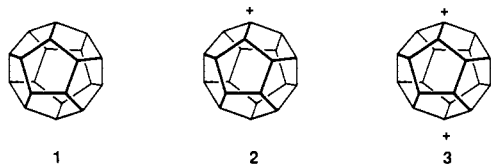
the highest possible point group symmetry ( $I_h$ , icosahedral), has been successfully met in two laboratories.<sup>3,4</sup> As more practical

<sup>†</sup> University of California.

<sup>‡</sup> The Ohio State University.

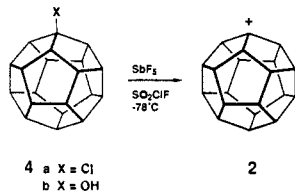
(1) (a) Considered as Stable Carbocations, Part 275, at the University of Southern California. (b) The Ohio State University Postdoctoral Fellow, 1986-1988.

and improved methods are becoming available for its preparation,<sup>5</sup> efforts are being directed toward effective functionalization of the dodecahedrane skeleton. Recently at Ohio State University<sup>5,6</sup> we defined, for the first time, various protocols capable of delivering a wide range of monofunctionalized dodecahedranes. The majority of this functionalization chemistry appears to rest on the transient generation and efficient trapping of the dodecahedryl monocation (**2**). In order to confirm this working hypothesis, we decided to generate and characterize **2** spectroscopically under long-lived stable ion conditions. In a preliminary communication,<sup>7</sup> we reported the direct NMR spectroscopic observation of **2** in superacidic solution as well as its remarkably facile conversion to the 1,16-dication **3**. In the present paper, we report full experimental details on the generation and observation of **2** and **3**. To understand their stability as well as their inability to undergo fast degenerate hydride shifts, we have also probed the structure of **2** and **3** theoretically at semiempirical SCF-MO levels.



### Results and Discussion

Dodecahedrane **1** and its derivatives **4a** and **4b** were available from previous work.<sup>5,6</sup> The ionizations were carried out in  $\text{SbF}_5/\text{SO}_2\text{ClF}$  solutions at  $-78^\circ\text{C}$  (dry ice-acetone). The  $^1\text{H}$  and  $^{13}\text{C}$  NMR spectra were recorded at 200 (also 500) and 50 MHz, respectively, over a temperature range of  $-70$  to  $0^\circ\text{C}$ . Assignments of  $^1\text{H}$  NMR signals were based on relative integrations and neighboring positive charge deshielding effects. The  $^{13}\text{C}$  NMR shifts were similarly assigned on the basis of relative intensity and by comparison with those of other carbocations. Quenching studies were carried out in methanol.



Dissolution of 5 mg of chlorododecahedrane (**4a**)<sup>5</sup> in 1 mL of  $\text{SO}_2\text{ClF}$  containing ca. 250 mg of  $\text{SbF}_5$  at  $-78^\circ\text{C}$  in a 5-mm NMR tube gave a pale yellow solution. At 200 MHz, the  $^1\text{H}$  NMR spectrum of this solution indicated a set of three absorptions at  $\delta$  4.64 (br, 3 H), 3.05 (br, 7 H), and 2.59 (br, 9 H). It was not possible to resolve the individual broad peaks even at a field strength of 500 MHz. The observed 3:7:9 relative integral area of the three absorptions indicates that the apical hydrogen atom at the 16-position, which is farthest from the positive charge, experiences more deshielding ( $\delta$  3.05) than the other belt hydrogens ( $\delta$  2.59), which are much closer to the positive charge. The  $^{13}\text{C}$  NMR spectrum at 50 MHz (Figure 1) consists of six absorptions at  $\delta$  363.9 (s), 81.1 (d), 64.4 (d), 64.1 (d), 63.0 (d), and 60.9 (d),

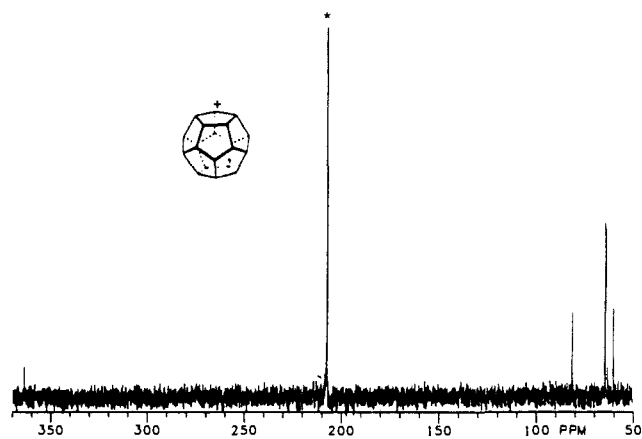


Figure 1. 50-MHz proton-decoupled  $^{13}\text{C}$  NMR spectrum of dodecahedryl cation (**2**) in  $\text{SbF}_5/\text{SO}_2\text{ClF}$  at  $-70^\circ\text{C}$ . \*: Carbonyl signal of the lock solvent acetone- $d_6$ .

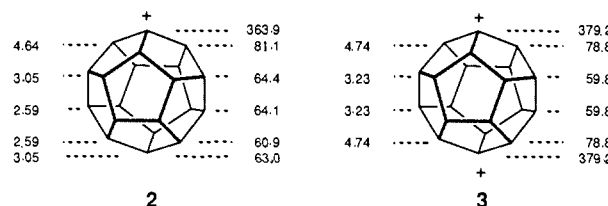


Figure 2. NMR chemical shift assignments of dodecahedryl cations **2** and **3**. Proton values are shown on the right and carbon data on the left.

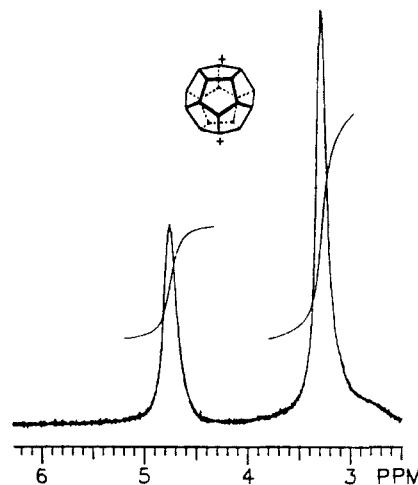
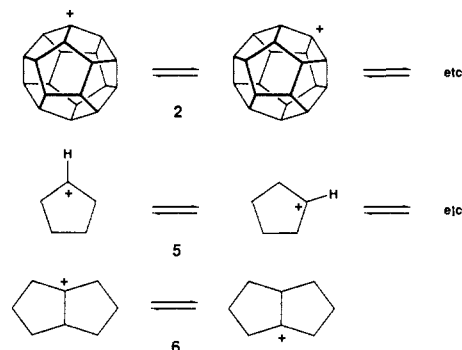


Figure 3. 200 MHz  $^1\text{H}$  NMR spectrum of 1,16-dodecahedryl dication (**3**) in  $\text{SbF}_5/\text{SO}_2\text{ClF}$  at  $-70^\circ\text{C}$ .

the assignments to which are shown in Figure 2. These observations clearly indicate the formation of the static dodecahedryl cation (**2**). The ion **2** was similarly obtained by ionizing dodecahedranol **4b**,<sup>5,6</sup> although dissolution occurred more slowly. The parent hydrocarbon **1** also slowly ionizes in the superacid medium at  $0^\circ\text{C}$  to provide the static cation **2**.



(2) (a) Eaton, P. E. *Tetrahedron* **1979**, *35*, 2189–2223. (b) Paquette, L. A.; Doherty, A. M. *Polyquinane Chemistry, Reactivity and Structure: Concepts in Organic Chemistry*; Springer: Berlin, 1987; Vol. 26.

(3) (a) Ternansky, R. J.; Balogh, D. W.; Paquette, L. A. *J. Am. Chem. Soc.* **1982**, *104*, 4503–4504. (b) Paquette, L. A.; Ternansky, R. J.; Balogh, D. W.; Kentgen, G. *Ibid.* **1983**, *105*, 5446–5450.

(4) (a) Fessner, W.-D.; Murty, B. A. R. C.; Wörth, J.; Hunkler, D.; Fritz, H.; Prinzbach, H.; Roth, W. R.; Schleyer, P. v. R.; McEwen, A. B.; Maier, W. F. *Angew. Chem., Int. Ed. Engl.* **1987**, *26*, 452–453. (b) Prinzbach, H.; Fessner, W.-D. In *Organic Synthesis: Modern Trends*; Chizhov, O., Ed.; Blackwell Scientific: Oxford, 1987; p 23–42.

(5) Paquette, L. A.; Weber, J. C.; Kobayashi, T.; Miyahara, Y., preceding paper in this issue.

(6) Paquette, L. A.; Weber, J. C.; Kobayashi, T. *J. Am. Chem. Soc.* **1988**, *110*, 1303–1304.

(7) Olah, G. A.; Prakash, G. K. S.; Kobayashi, T.; Paquette, L. A. *J. Am. Chem. Soc.* **1988**, *110*, 1304–1305.

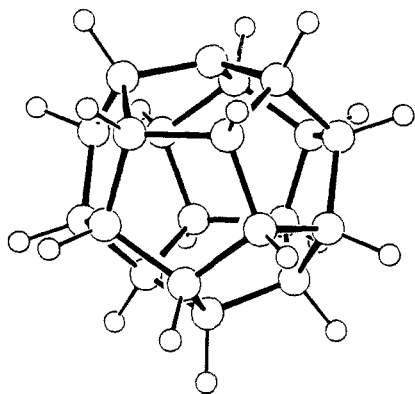
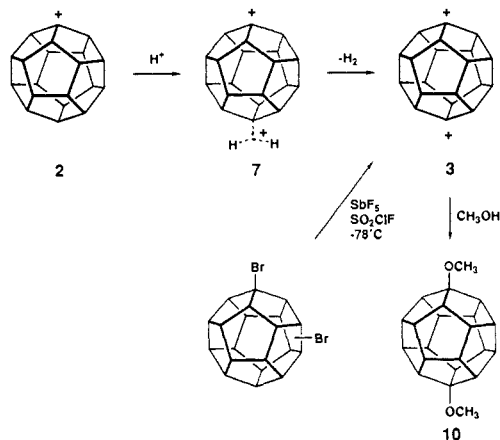


Figure 4. Calculated molecular structure of dodecahedryl cation (**2**) (MNDO).

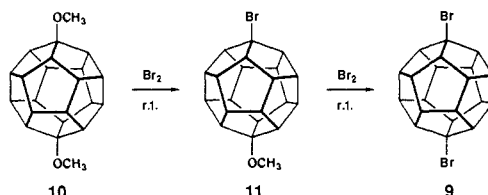
We expected that the dodecahedryl cation would undergo facile hydrogen scrambling through 1,2-hydride shifts similar to that observed in the related cyclopentyl (**5**)<sup>8</sup> and bicyclo[3.3.0]<sup>9</sup> cations (**6**), a process that would render all the carbon and hydrogen atoms equivalent for 20-fold degeneracy. However, no such degenerate rearrangements were observed, as indicated by the lack of change in the <sup>1</sup>H NMR line shapes, even when a solution of **2** was allowed to warm to 0 °C. Thus, the lower barrier for operation of such a degenerate rearrangement in **2** can be estimated to be approximately 15 kcal/mol. Additional considerations (vide infra) indicate that the barrier actually may not be much higher.

The dodecahedryl cation (**2**), upon standing in the superacidic medium for 6–7 h at –50 °C, is slowly and irreversibly transformed into a new species displaying simplified NMR spectra. Only two absorptions are observed at  $\delta$  4.74 (br, 6 H) and 3.23 (br, 12 H) in the 200-MHz proton NMR spectrum (see Figure 3) at –70 °C. The <sup>13</sup>C NMR spectrum indicates only three peaks at  $\delta$  379.2 (s), 78.8 (d), and 59.8 (d). These data allow the new species to be assigned as the *D*<sub>3d</sub>-symmetric 1,16-dodecahedryl dication (**3**) (cf. Figure 2). The formation of this unique, highly electron deficient dication can be rationalized by protolytic ionization<sup>10</sup> of the C–H bond at position 16 (farthest from the cationic center at position 1) involving a hypercarbon intermediate such as **7**.

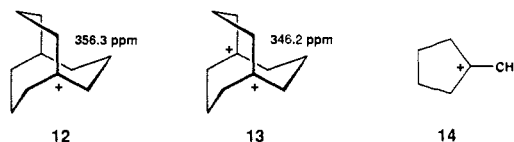


The structure of dication **3** was also confirmed by independent generation via the ionization of an isomeric mixture of dibromododecahedranes **8**, which is obtained by bromination of **1** in the presence of AlBr<sub>3</sub>. The dibromide mixture contains C<sub>20</sub>H<sub>18</sub>Br<sub>2</sub> components in the ratio of 5:6:2 (by GC–MS analysis) with the minor species being the 1,16-derivative **9** (vide infra). The independent conversion of **8** to **3** allows for ionization to occur

initially at the other available sites. The observation of only the 1,16-dication **3** as a static species suggests that 1,2-hydride shifts in the dodecahedrane skeleton occur readily, but they are still slow on the NMR time scale, once the cage is positively charged so as to position the positive charges as mutually distal as possible. The dication **3** was found to be rather stable at 0 °C for several days. Quenching of the solutions of this ion in methanol gave 1,16-dimethoxydodecahedrane (**10**) in  $\geq 85\%$  yield. This dimethoxy derivative, when treated with liquid bromine at room temperature, is slowly transformed into bromo ether **11** and ultimately into 1,16-dibromide **9**. The isomeric purity of these compounds appears to be 100% as checked by capillary GC. Thus, the ready preparation of dication **3** paves the way for effective regioselective functionalization of the dodecahedrane framework.



The <sup>13</sup>C chemical shifts of the positively charged centers in **2** ( $\delta$  363.9) and **3** ( $\delta$  379.2) happen to be the most deshielded ever observed for carbocationic species, indicating tremendous localization of the positive charge at these centers. Those previously recorded at the limit of the deshielding range include the 1-bicyclo[3.3.3]undecyl cation (**12**) and 1,5-bicyclo[3.3.3]undecadiyl dication (**13**).<sup>11</sup> Application of the <sup>13</sup>C chemical shift additivity criterion reveals a net deshielding of  $\delta$  283 for **2** and  $\delta$  610 for **3**, in agreement with progression from mono- to dication. However, the magnitude of deshielding per unit positive charge in both **2** and **3** is less than that observed in a typical tertiary carbocation such as the 1-methyl-1-cyclopentyl cation **14** ( $\Sigma\Delta = 374$  ppm).<sup>12</sup> This indicates the prevalence of some unique cage-shielding effect in the dodecahedryl cations, whose origin is difficult to specify due to the complexity of the multiple bond connectivities.



### Computational Analysis

The unanticipated properties of the dodecahedryl cations called for an evaluation of the underlying structural properties of these species. The experimental determination of alicyclic carbocation structures by X-ray crystallography is still limited, although methylated adamantyl<sup>13</sup> and norbornyl<sup>14</sup> cation structures have recently been elucidated successfully. In the crystalline state, the molecular structure is likely to be affected by the strong Coulombic interactions within an ionic crystal lattice. More accurate structural information for undisturbed geometries is likely to be expected from theoretical molecular-orbital calculations. Although systems as large as dodecahedrane (**1**) have been treated at ab initio levels of theory,<sup>15</sup> the systematic investigation of a larger set of derivatives and analogues of lower symmetry is not yet feasible. The Dewar semiempirical approximations,<sup>16</sup> however,

(11) Olah, G. A.; Liang, G.; Schleyer, P. v. R.; Parker, W.; Watt, C. I. *J. Am. Chem. Soc.* **1977**, *99*, 966–968.

(12) Schleyer, P. v. R.; Lenoir, D.; Mison, P.; Liang, G.; Prakash, G. K. S.; Olah, G. A. *J. Am. Chem. Soc.* **1980**, *102*, 683–691.

(13) Laube, T. *Angew. Chem.* **1986**, *98*, 368–369; *Angew. Chem., Int. Ed. Engl.* **1986**, *25*, 349–350.

(14) Laube, T. *Angew. Chem.* **1987**, *99*, 580–583; *Angew. Chem., Int. Ed. Engl.* **1987**, *26*, 560–561.

(15) (a) Schulman, J. M.; Disch, R. L. *J. Am. Chem. Soc.* **1984**, *106*, 1202–1204. (b) Disch, R. L.; Schulman, J. M.; Sabio, M. L. *Ibid.* **1985**, *107*, 1904–1906. (c) See also: Dixon, D. A.; Deerfield, D.; Graham, G. D. *Chem. Phys. Lett.* **1981**, *78*, 161–164. (d) Scamehorn, C. A.; Hermler, S. M.; Pitzer, R. M. *J. Chem. Phys.* **1986**, *84*, 833–837.

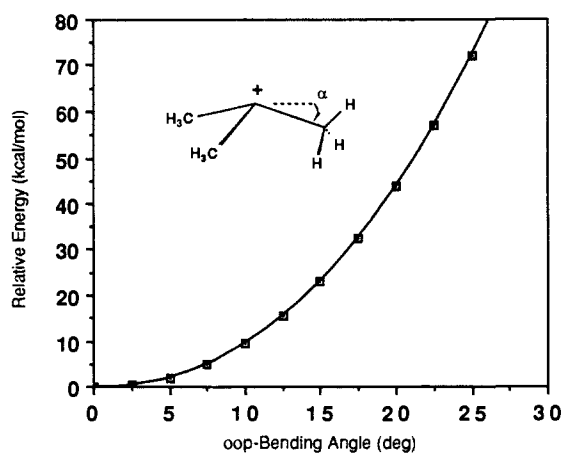
(8) (a) Olah, G. A.; Lukas, J. *J. Am. Chem. Soc.* **1967**, *89*, 4739–4744. (b) Brouwer, D. M.; Mackor, E. L. *Proc. Chem. Soc. (London)* **1964**, 147–153. (c) Brouwer, D. M. *Recl. Trav. Chim. Pays-Bas* **1968**, *87*, 210–212.

(9) Olah, G. A.; Liang, G.; Westerman, P. W. *J. Org. Chem.* **1974**, *39*, 367–369.

(10) Adventitious protic acid is invariably difficult to remove from such media.

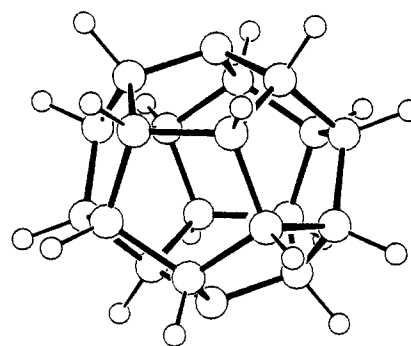
**Table I.** Selected Calculated Structure Data of Some Cage Hydrocarbons and Derived Cations

| compound                       | symmetry | C-C distance $d$ , Å |       |       | bending angle $\alpha$ , deg |      |      | pyramid. distance $h$ , Å |       |       | local charge on C <sup>+</sup> (MNDO) | cage diameter, Å (MNDO) |
|--------------------------------|----------|----------------------|-------|-------|------------------------------|------|------|---------------------------|-------|-------|---------------------------------------|-------------------------|
|                                |          | MNDO/3               |       |       | MNDO/3                       |      |      | MNDO/3                    |       |       |                                       |                         |
|                                |          | MNDO                 | AM1   | 3     | MNDO                         | AM1  | 3    | MNDO                      | AM1   | 3     |                                       |                         |
| dodecahedrane (1)              | $I_h$    | 1.555                | 1.534 | 1.565 | 20.9                         | 20.9 | 20.9 | 0.555                     | 0.548 | 0.559 |                                       |                         |
| dodecahedryl monocation (2)    | $C_{3v}$ | 1.497                | 1.475 | 1.512 | 11.1                         | 11.8 | 12.5 | 0.288                     | 0.302 | 0.327 | 0.40                                  |                         |
| 1,16-dodecahedryl dication (3) | $D_{3d}$ | 1.519                | 1.494 | 1.528 | 19.0                         | 18.9 | 19.0 | 0.494                     | 0.485 | 0.497 | 0.42                                  | 4.125                   |
| centrotriquinane               | $C_{3v}$ | 1.556                | 1.535 | 1.567 | 20.2                         | 20.6 | 20.2 | 0.538                     | 0.540 | 0.540 |                                       |                         |
| 1-centrotriquinyl cation (17)  | $C_{3v}$ | 1.492                | 1.471 | 1.507 | 9.3                          | 10.6 | 10.0 | 0.242                     | 0.271 | 0.262 | 0.38                                  |                         |
| adamantane                     | $T_d$    | 1.554                | 1.526 | 1.551 | 19.4                         | 19.5 | 19.6 | 0.517                     | 0.510 | 0.519 |                                       |                         |
| 1-adamantyl cation             | $C_{3v}$ | 1.499                | 1.468 | 1.493 | 9.3                          | 9.8  | 10.1 | 0.242                     | 0.249 | 0.269 | 0.33                                  |                         |
| diamantane                     | $D_{3d}$ | 1.551                | 1.525 | 1.545 | 19.6                         | 19.6 | 19.9 | 0.520                     | 0.511 | 0.527 |                                       |                         |
| 4-diamantyl cation             | $C_{3v}$ | 1.495                | 1.467 | 1.489 | 9.3                          | 9.8  | 10.6 | 0.241                     | 0.250 | 0.273 | 0.33                                  |                         |
| 4,9-diamantyl dication         | $D_{3d}$ | 1.502                | 1.474 | 1.494 | 9.4                          | 9.9  | 9.9  | 0.245                     | 0.253 | 0.258 | 0.37                                  | 4.207                   |
| manxane                        | $C_3$    | 1.551                | 1.522 | 1.542 | 13.1                         | 14.2 | 12.3 | 0.352                     | 0.374 | 0.329 |                                       |                         |
| 1-manxyl monocation (12)       | $C_3$    | 1.498                | 1.464 | 1.492 | 0.9                          | 1.3  | 2.5  | 0.023                     | 0.032 | 0.066 | 0.39                                  |                         |
| 1,5-manxyl dication (13)       | $D_{3h}$ | 1.505                | 1.468 | 1.498 | 1.8                          | 2.2  | 2.6  | 0.048                     | 0.056 | 0.069 | 0.37                                  | 2.761                   |

**Figure 5.** Bending potential of *tert*-butyl cation (15) for  $C_{3v}$ -symmetrical distortion (MNDO).

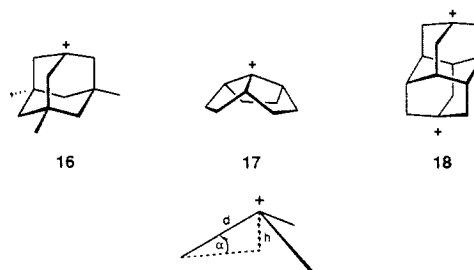
have been documented to provide relatively fast access to satisfactory geometry and energy data.<sup>16,17</sup> While the accuracy of AM1 has not yet been as widely assessed, the well-established MNDO Hamiltonian has recently been shown to reproduce exceptionally well the structural features of related complex polycyclics such as pagodanes.<sup>18</sup> The comparison of calculated values for uncharged dodecahedrane (Table I) with those recently determined experimentally for the parent compound<sup>19</sup> and a dimethyl derivative<sup>20</sup> further attests to this.

Equilibrium geometries for the dodecahedryl mono- and dications **2** and **3** were determined with retention of the highest possible point-group symmetries of  $C_{3v}$  and  $D_{3d}$ , respectively. While the majority of its structure is hardly affected by the electron deficiency, monocation **2** exhibits considerable deformation around the cationic center, as expected from the preference of cations to adopt a planar  $sp^2$  geometry (Figure 4). Complete planarization, however, is precluded within the spherical framework as a direct consequence of the simultaneous increase in

**Figure 6.** Calculated molecular structure of dodecahedryl 1,16-dication **3** (MNDO).

bond-angle distortion at the adjacent tetrahedral centers. These forces are balanced in **2** at a pyramidalization level of about  $11^\circ$ , expressed as the out-of-plane (oop) bending angle of the central atom relative to the plane defined by its three bonding partners.<sup>21</sup> For comparison, the corresponding value for a regular  $sp^3$ -hybridized corner in dodecahedrane is close to  $21^\circ$ .

The calculated bending potential of the *tert*-butyl cation (**15**, Figure 5), when fixed to a comparable  $C_{3v}$  symmetry, allows a rough estimate to be made as to the relative energy required for this particular type of distortion. Table I contains a synopsis of calculated data for some related (hemi)spherical cations. The situation calculated for **2** compares nicely with the structure of the bridgehead 3,5,7-trimethyladamantyl cation **16**, which has



recently been determined by X-ray analysis<sup>13</sup> (oop-deviation  $9^\circ$ ). In contrast to the electronic situation in adamantyl cations,<sup>22</sup> the  $\beta$ -bonds in the dodecahedryl cation (**2**) are inadequately oriented to stabilize the empty p orbital by C-C hyperconjugation, with a dihedral angle close to  $90^\circ$ . Somewhat surprisingly, the three better aligned  $\beta$ -C-H bonds are predicted to be actually bent away from the charged carbon with a C<sup>+</sup>-C-H angle of  $115^\circ$ , presumably due to the total of angle deformations at these carbon atoms. In the geometry of the more flexible centrotriquinane

(16) (a) MNDO/3: Bingham, R. C.; Dewar, M. J. S.; Lo, D. H. *J. Am. Chem. Soc.* **1975**, *97*, 1285-1293. (b) MNDO: Dewar, M. J. S.; Thiel, W. *Ibid.* **1977**, *99*, 4899-4907. (c) AM1: Dewar, M. J. S.; Zoebisch, E. G.; Healy, E. F.; Stewart, J. J. P. *Ibid.* **1985**, *107*, 3902-3909.

(17) (a) Dewar, M. J. S.; Ford, G. P. *J. Am. Chem. Soc.* **1979**, *101*, 5558-5561. (b) Dewar, M. J. S.; Storch, D. M. *Ibid.* **1985**, *107*, 3898-3902.

(18) (a) Fessner, W.-D.; Sedelmeier, G.; Spurr, P. R.; Rihs, G.; Prinzbach, H. *J. Am. Chem. Soc.* **1987**, *109*, 4626-4642. (b) Prakash, G. K. S.; Kirshnamurthy, V. V.; Herges, R.; Bau, R.; Yuan, H.; Olah, G. A.; Fessner, W.-D.; Prinzbach, H. *Ibid.*, in press.

(19) Gallucci, J. C.; Doecke, C. W.; Paquette, L. A. *J. Am. Chem. Soc.* **1986**, *108*, 1343-1344. The average bond length of 1.538 Å seems to be somewhat short in view of the average value of 1.545 Å determined for bonds between tertiary centers in the 1,16-dimethyl derivative<sup>20</sup> and might reflect complications that arose from crystal twinning. For additional discussion on this issue, consult: Gallucci, J. C.; Taylor, R. T.; Kobayashi, T.; Weber, J. C.; Krause, J.; Paquette, L. A. *Acta Crystallogr.*, in press.

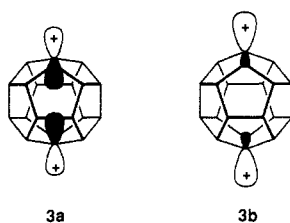
(20) (a) Christoph, G. G.; Engel, P.; Usha, R.; Balogh, D. W.; Paquette, L. A. *J. Am. Chem. Soc.* **1982**, *104*, 784-791. (b) Allinger, N. L.; Geise, H. J.; Pyckhout, W.; Paquette, L. A.; Gallucci, J. C. *Ibid.*, in press.

(21) We prefer the usage of this notation rather than that of the distance from the plane as is commonly used by crystallographers,<sup>13</sup> since the angle is independent of variations in bond distances.

(22) Sunko, D. E.; Hirsl-Starcevic, S.; Pollack, S. K.; Hehre, W. J. *J. Am. Chem. Soc.* **1979**, *101*, 6163-6170.

apical cation **17** ( $C_{3v}$ ), which can be regarded as a section of the dodecahedrane framework, the reduced oop angle confirms the predominant influence of a convex bonding nature, whereas the minor structural restrictions and relief of angle strain in the manxyl cation (**12**) allow for an almost complete flattening.

With its substantially smaller deviations from full dodecahedrane symmetry and an oop angle of  $19^\circ$ , the 1,16-dication structure (**3**) incorporates almost perfectly  $sp^3$ -hybridized centers of unsaturation (Figure 6). The  $\alpha$ -bonds are relatively long for a carbocation with 1.519 Å. In contrast to other known spherical dications that are sufficiently stabilized by C–C hyperconjugation, e.g. the 1,9-diamantyl (**18**)<sup>23</sup> or 1,5-manxyl (**13**)<sup>11</sup> dications (Table I), the two charges are much less dispersed among the dodecahedrane carbon framework. In consequence of the empty internal cavity of the sphere, an assumed  $sp^2$ -hybridized dication depicted by **3a** with planar geometry around the cationic centers would enforce strong Coulombic charge repulsion and through-space interaction of the nonbonding p lobes, whereas in **3b** an enlarged



transannular distance and outward directed  $sp^3$  orbitals alleviate those unfavorable interactions. In line with experimental deshielding effects, the positive charge is more strongly localized on the respective carbon atoms relative to the other cations in Table I.

Consideration was also given to the underlying cause of the unanticipatedly high barrier for degenerate H migration, although 1,2 shifts in carbenium ions are generally facile processes.<sup>24</sup> Basically, there are two possible reasons for an increase of the reaction barrier: either the ground-state geometry is inappropriate for a migration to occur or the transition state is energetically unfavorable. Although extensive data, up to highest theoretical levels, have been accumulated in recent years on simple alkyl cations, the majority focuses only on the determination of relative stabilities of classical and hydrogen-bridged forms,<sup>25</sup> and detailed investigations relevant to a dependency of hydride shifts on geometrical constraints and associated hybridization states are uncommon. For example, Chandrasekhar and Schleyer have demonstrated that the effect of ring size on 1,2-shift barriers in simple cyclic cases is caused mainly by development of angle strain on the way to the transition state.<sup>26</sup>

For dodecahedryl cations, the argument of an unfavorable ground-state geometry does not hold, since the empty p orbital in fact is perfectly aligned with the migrating C–H bond in a coplanar fashion, with the 3-fold degeneracy as additional statistical advantage. The distance between the  $C^+ \cdots H$  reaction centers is somewhat larger at 2.209 Å relative to the  $sp^2$ -hybridized 2,3-dimethyl-2-butyl cation (**19**) as a model (2.067 Å, cf. Table II). This phenomenon arises because of the above-noted distortions of bond angle and bond lengths and is in line with a diminished orbital interaction due to pyramidalization at  $C^+$  (cf. Scheme II), although this constitutes only a small contribution to the overall effect.

The influence of  $C_{2v}$ -symmetric oop bending on the transition-state energy was modelled first on **19**, the tetramethylated

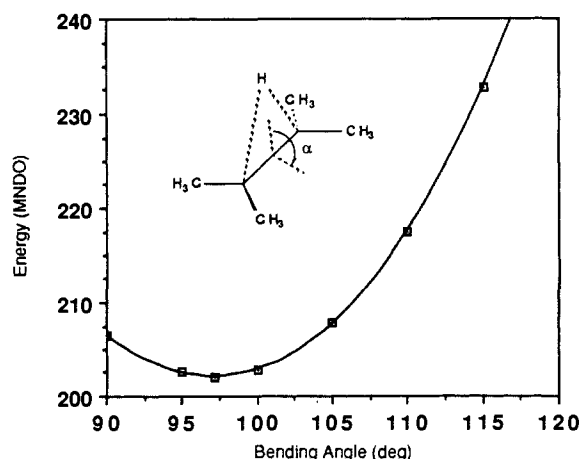
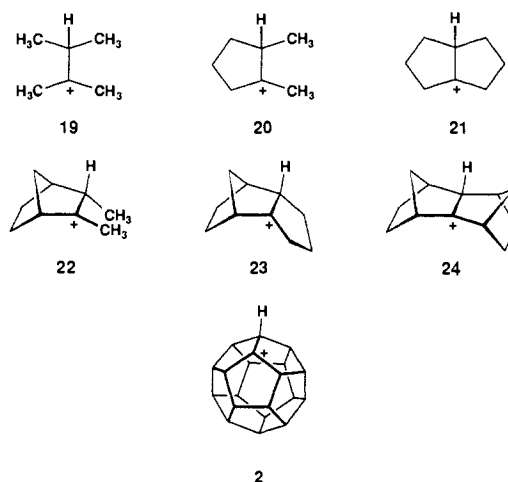


Figure 7. Bending potential of 2,3-dimethyl-2-butyl cation (**19**)  $C_{2v}$  symmetry (MNDO).

Scheme I. Structure Set Considered for Calculation of Hydride-Shift Barriers



system being chosen instead of the usually studied parent ethyl cation in order to encompass the stronger torsional effects stemming from carbon substitution. Figure 7 illustrates the bending force field as derived from the MNDO results that reveals an energy minimum for a  $7^\circ$  deviation of the carbon skeleton from planarity, in agreement with the view that the TS is an olefin-proton  $\pi$ -complex. As the situation gets closer to the range of interplanar angles required for the fusion of cyclopentane rings, the potential energy steeply increases.

For the seven systems (**2** and **19–24**) displayed in Scheme I, which incorporate the partial structure **19** and for which experimental determinations are available,<sup>11,27–29</sup> barriers for hydride shifts were next calculated. The selection was restricted to tertiary cations and to quinane structures to exclude a ring-size effect.<sup>26</sup> Assuming planar symmetry for all bridged transition states and for classical structures where available, all remaining structural degrees of freedom were fully optimized. Heats of formation and some selected structural features obtained with the different semiempirical methods are compiled in Table II; the energy differences between ground and transition states, which represent the height of the reaction barrier, are compared to experimental values derived from dynamic NMR measurements. Corrections are made relative to the simplest representative (**19**) as reference point; they result from the different capability of the methods to

(23) Olah, G. A.; Prakash, G. K. S.; Shih, J. G.; Krishnamurthy, V. V.; Mateescu, G. D.; Liang, G.; Sipos, G.; Buss, V.; Gund, T. M.; Schleyer, P. v. R. *J. Am. Chem. Soc.* **1985**, *107*, 2764–2772.

(24) Saunders, M.; Chandrasekhar, J.; Schleyer, P. v. R. *Rearrangements in Ground and Excited States*; Mayo, P. D., Ed.; Academic: New York, 1980; Vol. 1, p 1.

(25) Hehre, W. J.; Radom, L.; Schleyer, P. v. R.; Pople, J. A. *Ab Initio Molecular Orbital Theory*; Wiley Interscience: New York, 1986 and references cited therein.

(26) Chandrasekhar, J.; Schleyer, P. v. R. *Tetrahedron Lett.* **1979**, 4057–4060.

(27) Saunders, M.; Kates, M. R. *J. Am. Chem. Soc.* **1978**, *100*, 7082–7083.

(28) (a) Jones, A. J.; Huang, E.; Haseltine, R.; Sorensen, T. S. *J. Am. Chem. Soc.* **1975**, *97*, 1133–1139. (b) Sorensen, T. S. *Acc. Chem. Res.* **1976**, *9*, 257–265.

(29) Paquette, L. A.; DeLuca, G.; Ohkata, K.; Gallucci, J. C. *J. Am. Chem. Soc.* **1985**, *107*, 1015–1023.

**Table II.** Calculated Heats of Formation and Selected Structure Data of Classical and Hydrogen-Bridged Cations; Comparison between Calculated Hydride-Shift Barriers (Corrected for Systematic Methodic Errors) and Experimental Activation Energies

| com-<br>pound | sym-<br>metry | H...C <sup>+</sup> distance d(Å) |       |       |       | $\Delta H_f^\circ$ , kcal/mol |       |       |       | $\Delta\Delta H_f^\circ$ , cor., kcal/mol |       |       |       | exptl<br>$\Delta G^\ddagger$<br>ref |    |
|---------------|---------------|----------------------------------|-------|-------|-------|-------------------------------|-------|-------|-------|---|-------|-------|-------|-------------------------------------|----|
|               |               | MINDO/3                          |       | AMI   |       | MINDO/3                       |       | AMI   |       | MINDO/3                                   |       | AMI   |       |                                     |    |
|               |               | MINDO                            | AMI   | MINDO | AMI   | MINDO                         | AMI   | MINDO | AMI   | MINDO                                     | AMI   | MINDO | AMI   |                                     |    |
| 19            | classical     | 2.067                            | 2.068 | 1.793 | 162.8 | 183.6                         | 167.7 | 15.9  | 0.00  | 0.00                                      | 0.00  | 0.00  | 0.00  | 3.1                                 | 27 |
|               | bridged TS    | 1.386                            | 1.413 | 1.309 | 178.7 | 202.2                         | 166.4 | 16.8  | 2.13  | 2.13                                      | 2.13  | 0.91  | 0.63  | 3.1                                 | 27 |
| 20            | classical     | 2.092                            | 2.099 | 1.929 | 162.5 | 175.7                         | 162.1 | 16.8  | 2.13  | 2.13                                      | 2.13  | 0.91  | 0.63  | 3.1                                 | 27 |
|               | bridged TS    | 1.390                            | 1.415 | 1.310 | 179.3 | 196.4                         | 162.1 | 20.2  | 6.76  | 6.76                                      | 6.76  | 4.32  | 4.09  | 4.0                                 | 11 |
| 21            | classical     | 2.159                            | 2.094 | 2.094 | 169.8 | 178.7                         | 168.8 | 20.2  | 6.76  | 6.76                                      | 6.76  | 4.32  | 4.09  | 4.0                                 | 11 |
|               | bridged TS    | 1.396                            | 1.421 | 1.315 | 190.0 | 204.1                         | 171.5 | 18.9  | 5.82  | 5.82                                      | 5.82  | 3.03  | 3.95  | 6.6                                 | 28 |
| 22            | classical     | 2.135                            | 2.114 | 2.023 | 179.6 | 194.4                         | 195.0 | 18.9  | 5.82  | 5.82                                      | 5.82  | 3.03  | 3.95  | 6.6                                 | 28 |
|               | bridged TS    | 1.392                            | 1.418 | 1.313 | 198.5 | 218.8                         | 197.6 | 23.5  | 11.18 | 11.18                                     | 11.18 | 7.64  | 8.56  | 7.2                                 | 23 |
| 23            | classical     | 2.201                            | 2.183 | 2.168 | 188.0 | 200.9                         | 203.1 | 23.5  | 11.18 | 11.18                                     | 11.18 | 7.64  | 8.56  | 7.2                                 | 23 |
|               | bridged TS    | 1.399                            | 1.423 | 1.320 | 211.6 | 230.6                         | 210.3 | 23.4  | 12.86 | 12.86                                     | 12.86 | 7.48  | 10.75 | 7.0                                 | 29 |
| 24            | classical     | 2.259                            | 2.205 | 2.207 | 211.9 | 230.3                         | 242.5 | 23.4  | 12.86 | 12.86                                     | 12.86 | 7.48  | 10.75 | 7.0                                 | 29 |
|               | bridged TS    | 1.404                            | 1.434 | 1.323 | 251.9 | 261.8                         | 251.9 | 33.6  | 19.75 | 19.75                                     | 19.75 | 17.70 | 17.45 | 15.0                                | 7  |
| 2             | classical     | 2.209                            | 2.201 | 2.197 | 182.4 | 178.3                         | 278.1 | 33.6  | 16.1  | 16.1                                      | 16.1  | 17.70 | 17.45 | 15.0                                | 7  |
|               | bridged TS    | 1.382                            | 1.398 | 1.309 | 216.0 | 216.7                         | 294.2 |       |       |   |       |       |       |                                     |    |

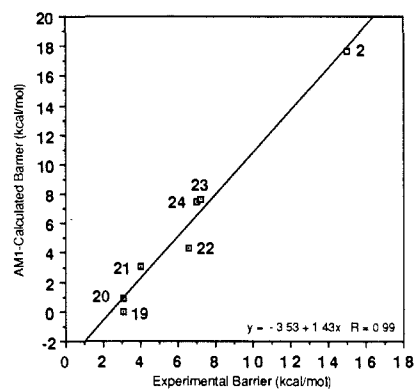
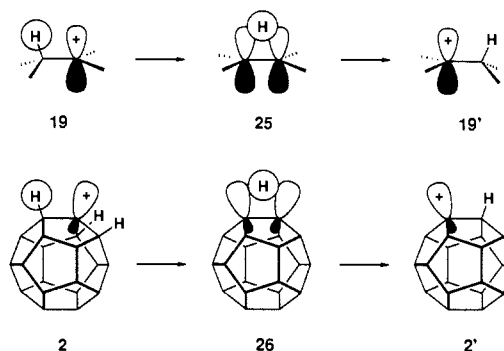


**Figure 8.** Correlation of experimental and calculated activation energies for cations **2** and **19–24** (AM1).

**Scheme II.** Localized Orbital Interactions in Hydride Shifts of Planar and Distorted Carbocations



estimate the energy content of bridged species. The accuracy of *absolute* energy values and differences is not of concern here as we are only interested in the *trend for relative energy differences within the series*. Attention is drawn to the fact that systematic differences have to be expected because the enthalpy differences are calculated for isolated molecules in the gas phase, while experimental results refer to measurements in solution under stable-ion conditions. The validity of this approach is enhanced by the fact that all three methods employed give essentially identical results.

Figure 8 demonstrates that the calculated values parallel the experimental determinations quite closely, especially when one takes into consideration that the experimental data, particularly on the lower end of the scale, are associated with some methodological ambiguities.<sup>30</sup> The somewhat larger deviations implied for the 2,3-dimethyl-2-norbornyl cation (**22**) and the *syn,endo*-sesquinorbornyl cation (**24**) might reflect a deficiency of the semiempirical methods in reproducing correctly the torsional effects in norbornene-type systems, as has been pointed out recently for MNDO by Brown and Houk.<sup>31</sup> Possible effects of nonclassical stabilization (bridging, C–C hyperconjugation) for norbornane systems are at least partially accounted for by the MO treatments.<sup>32</sup> The best fit to experimental values is obtained with AM1, which has been properly parameterized to account for hydrogen bridging.<sup>16</sup>

In Scheme II an attempt is made to illustrate our rationale for the effect by comparison of a generic, acyclic cation (**19**) to the spherically bent dodecahedryl cation, **2**. Clearly, in TS **26** the

(30) The calculated barrier for an endo-hydride shift in 2,3-dimethyl-2-norbornyl cation of 3.4 kcal/mol (from MINDO/3, corrected to be 4.7 kcal/mol; 26.3 kcal/mol from MNDO, corrected to be 7.7 kcal/mol) is in contrast to estimates of Sorensen et al.<sup>28</sup> for a lower limit of 12 kcal/mol. As the latter estimates are derived only from negative experimental evidence in a complex 2-norbornyl system, we feel unable to validate the computational predictions for this case.

(31) Brown, F. K.; Houk, K. N. *J. Am. Chem. Soc.* **1985**, *107*, 1971–1978.

(32) Montgomery, L. K.; Grendze, M. P. *12th Austin Symposium on Molecular Structure*, Feb 28–Mar 2, 1988; Abstract TM5.

stabilizing overlap between the diffuse hydrogen s orbital and the bent, outward directed  $sp^2$ -type carbon orbitals is weaker relative to an interaction with the more obtuse p orbitals in **25**. Consideration of the transition state as representing a protonated olefin warrants that the classical torsional strain in dodecahedrene also be considered a plausible cause. For the strongly distorted double bond in dodecahedrene an oop-bending angle of  $46.5^\circ$  and a strain value of 87.3 kcal/mol (18.3 kcal/mol relative to dodecahedrane **1**) have been calculated with the MM2 force field.<sup>33</sup> Recently, dodecahedrene has been generated as the neutral product of ion-molecule reactions performed in an FT-ICR mass spectrometer.<sup>34</sup> From the thermochemistry associated with the observed reactions, the heat of hydrogenation of dodecahedrene was indirectly shown to be  $40 \pm 3$  kcal/mol more negative than that of ethylene, a value indicating that its olefinic carbons possess nearly tetrahedral geometry. For this reason, a linear relationship between hydride-shift barriers and the empirically defined olefin strain, as proposed for bridgehead olefins by Maier and Schleyer,<sup>35</sup> can be assumed. Further work in this direction is in progress.

### Conclusions

Our NMR spectroscopic and theoretical studies on dodecahedryl cation (**2**) and 1,16-dication **3** reveal several interesting characteristics of the dodecahedrane cage. More charge seems to be localized at the cationic centers in both species as compared to other bridgehead cations, reflecting the inability of the cage geometry to accommodate an almost flat  $sp^2$ -hybridized geometry around the unsaturated carbon, as well as a lack of significant C-C-hyperconjugative stabilization. This effect appears to be more severe for the doubly charged dication **3** than for the monocation **2**. At the computational levels applied, the cationic centers in **3** feature an almost unperturbed  $sp^3$ -hybridized state with outward oriented empty orbitals. Obviously, through-space repulsive electrostatic effects are strong enough to outweigh the energetic demands of bending. In contrast to the situation calculated for isolated molecules, such a constitution may also benefit from ion-pairing effects with respective gegenions in solution. However, the result of total shielding per unit of positive charge observed for both dodecahedryl cations by additivity relationship remains unexplained. The effect may be partially due to the multitude of bond connectivities in the cage.

The lack of facile degenerate hydrogen scrambling in **2** (estimated barrier  $\geq 15$  kcal/mol), in spite of excellent alignment of migrating C-H bonds, is explained by the crucial influence of convex bending within the bridged transition state. Strong Coulombic forces probably further enhance the static nature of the dication **3** relative to **2**.

Finally, the ease of formation of dication **3** from **2** (and ultimately from **1**) in a regiospecific manner opens up the possibility for the selective 1,16-difunctionalization of the dodecahedrane sphere.

### Experimental Section

**General Procedures.** Dodecahedrane **1** and its derivatives **4** were available from previous studies.<sup>5,6</sup>  $^1\text{H}$  and  $^{13}\text{C}$  NMR spectra were recorded on either a Varian Associates Model VXR-200 NMR spectrometer equipped with a 5-mm broad-band variable-temperature probe or a

Bruker WM-300 NMR spectrometer (300 MHz) at OSU. Mass spectral analyses were obtained with a Kratos MS-30 instrument operating at 70 eV. Melting points are uncorrected.

**Preparation of Cations.** Dissolution of  $\sim 5$  mg of chlorododecahedrane **4a** into a mixture of  $\text{SbF}_5/\text{SO}_2\text{ClF}$  (1 mL  $\text{SO}_2\text{ClF}$  containing ca. 250 mg of freshly distilled  $\text{SbF}_5$ ) at  $-78^\circ\text{C}$  gave a pale yellow solution. Initially the dodecahedryl monocation was formed, which was slowly transformed into the dication (over a period of approximately 6–7 h at  $-50^\circ\text{C}$  under the above conditions). The ionization of **1**, **4a**, and **4b** was carried out similarly, but the former two compounds required higher temperatures ( $-30$  to  $-10^\circ\text{C}$ ).

**Methanol Quenching of Dication 3.** The solution of dodecahedryl dication **3**, prepared as described above, was rapidly treated with 5 mL of precooled, dry methyl alcohol at  $-78^\circ\text{C}$ , followed by addition of 2 g of solid sodium bicarbonate and 20 mL of ice water. The mixture was repeatedly extracted with dichloromethane ( $3 \times 40$  mL), and the combined extracts were washed with water ( $3 \times 60$  mL) and dried over  $\text{MgSO}_4$ . Evaporation provided a colorless solid which contained  $\geq 85\%$  1,16-dimethoxydodecahedrane (**10**). Pure **10** was obtained by preparative TLC on silica gel (elution with 20% ethyl acetate in petroleum ether); colorless crystals, mp  $247\text{--}248^\circ\text{C}$  (from hexane/benzene, 2:10); 6.1 mg (72%); IR ( $\text{CHCl}_3$ ,  $\text{cm}^{-1}$ ) 3003, 2946, 1333, 1324, 1312, 1295, 1247, 1075, 960;  $^1\text{H}$  NMR (300 MHz,  $\text{CDCl}_3$ )  $\delta$  3.50 (br s, 12 H), 3.42 (br s, 6 H), 3.24 (s, 6 H);  $^{13}\text{C}$  NMR (75 MHz,  $\text{CDCl}_3$ )  $\delta$  122.3, 67.8, 65.5, 51.3; MS,  $m/z$  ( $M^+$ ) calcd 320.1786, obsd 320.1781.

**Dibromododecahedranes (8).** A solution of bromododecahedrane (**7** mg) in 5 mL of liquid bromine was treated with aluminum bromide (ca. 10 mg) and heated while magnetically stirred at  $55^\circ\text{C}$  for 18 h. After cooling, the excess bromine was evaporated in vacuo, the residue was treated with ice water, and the products were extracted into dichloromethane. Drying and solvent removal furnished a residue (9 mg) constituted of three  $\text{C}_{20}\text{H}_{18}\text{Br}_2$  components (GC-MS analysis) in the ratio of 5:6:2 with the minor constituent being **9**. The relative positions of the pair of bromine atoms in the two dominant products has not been determined due to an inability to separate the three-component mixture.

**1-Bromo-16-methoxydodecahedrane (11).** A solution of **10** (11 mg, 34.3  $\mu\text{mol}$ ) in liquid bromine (5 mL) was stirred at room temperature for 24 h. The excess bromine was blown off under a stream of argon. The residue was separated into its components by preparative TLC on silica gel (elution with 5% ethyl acetate in petroleum ether). There was isolated 1.7 mg (12%) of dibromide **9**, 2.0 mg (22%) of **11**, and 2.8 mg (25%) of recovered **10**.

For **11**: colorless solid, mp  $>250^\circ\text{C}$ , (from hexane); IR ( $\text{CHCl}_3$ ,  $\text{cm}^{-1}$ ) 2956, 1193;  $^1\text{H}$  NMR (300 MHz,  $\text{CDCl}_3$ )  $\delta$  3.95–3.83 (m, 3 H), 3.75–3.35 (m, 15 H), 3.22 (s, 3 H);  $^{13}\text{C}$  NMR (125 MHz,  $\text{CDCl}_3$ )  $\delta$  78.8, 68.1, 65.7, 65.0, 51.3 (two quaternary carbons not observed); MS,  $m/z$  ( $M^+$ ) calcd 370.0756, obsd 370.0743.

**1,16-Dibromododecahedrane (9).** A solution of **10** (3.0 mg, 9.3  $\mu\text{mol}$ ) was treated with bromine (5 mL) and stirred at room temperature for 4 days. The excess bromine was blown off under a stream of argon and the residual solid was purified by passage through a short plug of silica gel (elution with 5% ethyl acetate in petroleum ether). There was isolated 2.3 mg (59%) of **9** as a colorless solid, mp  $>270^\circ\text{C}$  (from hexane/benzene, 4:1); IR ( $\text{CHCl}_3$ ,  $\text{cm}^{-1}$ ) 2928, 1192;  $^1\text{H}$  NMR (300 MHz,  $\text{CDCl}_3$ )  $\delta$  3.93 (br s, 6 H), 3.60 (br s, 12 H);  $^{13}\text{C}$  NMR (125 MHz,  $\text{CDCl}_3$ )  $\delta$  95.6, 79.1, 65.3; MS,  $m/z$  ( $M^+$ ) calcd 417.9754, obsd 417.9727.

**Acknowledgment.** Support by the National Institutes of Health of the work at both USC and OSU is gratefully acknowledged. Professor F. A. L. Anet is thanked for a 500-MHz  $^1\text{H}$  NMR spectrum.

**Supplementary Material Available.** Z matrices and Cartesian coordinates of optimized geometries for molecules in Tables I and II are available from one of the authors (W.-D.F.)<sup>36</sup> upon request.

(36) Address requests to this author at Institut für Organische Chemie, Universität Freiburg, Albertstr. 21, D-7800 Freiburg i.Br.; FRG.

(33) Fessner, W.-D. Ph.D. Thesis, Universität Freiburg, 1986.

(34) Kiplinger, J. P.; Marshall, A. G.; Kobayashi, T.; Paquette, L. A., submitted for publication.

(35) Maier, W. F.; Schleyer, P. v. R. *J. Am. Chem. Soc.* **1981**, *103*, 1891–1900.